

Does fluoride disrupt hydrogen bond network in cationic lipid bilayer? Time-dependent fluorescence shift of Laurdan and MD simulations

Sarka Pokorna,¹ Piotr Jurkiewicz,¹ Mario Vazdar,² Lukasz Cwiklik,^{1,3} Pavel Jungwirth,^{3,4} Martin Hof^{1,a)}

¹ J. Heyrovský Institute of Physical Chemistry of the Academy of Sciences of the Czech Republic v.v.i., Dolejskova 3, 18223 Prague 8, Czech Republic,

² Division of Organic Chemistry and Biochemistry, Rudjer Bošković Institute, P.O.B. 180, HR-10002 Zagreb, Croatia,

³ Institute of Organic Chemistry and Biochemistry, Academy of Sciences of the Czech Republic, Flemingovo nám. 2, 16610 Prague 6, Czech Republic

⁴ Department of Physics, Tampere University of Technology, P.O. Box 692, FI-33101 Tampere, Finland

^{a)} Author to whom correspondence should be addressed: martin.hof@jh-inst.cas.cz

ABSTRACT

Time-dependent fluorescence shift (TDFS) of Laurdan embedded in phospholipid bilayers reports on hydration and mobility of the phospholipid acylgroups. Exchange of H₂O with D₂O prolongs the lifetime of lipid-water and lipid-water-lipid interactions, which is reflected in a significantly slower TDFS kinetics. Combining TDFS measurements in H₂O or D₂O hydrated bilayers with atomistic molecular dynamics (MD) simulations provides a unique tool for characterization of the hydrogen bonding at the acylgroup level of lipid bilayers. In this work, we use this approach to study the influence of fluoride anions on the properties of cationic bilayers composed of trimethylammonium-propane (DOTAP). The results obtained for DOTAP are confronted with those for neutral phosphatidylcholine (DOPC) bilayers. Both in DOTAP and DOPC H₂O/D₂O exchange prolongs hydrogen-bonding lifetime and does not disturb bilayer structure. These results are confirmed by MD simulations. TDFS experiments show, however, that for DOTAP this effect is cancelled in the presence of fluoride ions. We interpret these results as evidence that strongly hydrated fluoride is able to steal water molecules that bridge lipid carbonyls. Consequently, when attracted to DOTAP bilayer, fluoride disrupts the local hydrogen-bonding network, and the differences in TDFS kinetics between H₂O and D₂O hydrated bilayers are no longer observed. A distinct behavior of fluoride is also evidenced by MD simulations, which show different lipid-ion binding for Cl⁻ and F⁻.

I. INTRODUCTION

A. Heavy water in biology: Importance of hydrogen bonds

For biomolecules, the presence of a surrounding aqueous medium is fundamental for acquiring proper structure and function. Biological systems are very sensitive to even small changes in solvent properties. Deuterium is twice as heavy as protium. Consequently, there is a number of minor differences in the physicochemical characteristics of light and heavy water (e.g. see the review of Nemethy & Scheraga¹ and references therein). Higher density, viscosity, as well as melting and boiling points of D₂O indicate its more tightly bound structure, nevertheless H₂O and D₂O are still very similar. Still, exchange of H₂O with D₂O affects various biological processes, e.g., length of circadian oscillation,^{2,3} formation of red blood cells,^{4,5} and formation of mitotic spindle^{4,6}. Exchange of more than 20% of body weight by heavy water can be toxic for eukaryotes, while algae and bacteria can adapt even to pure D₂O.⁴ H/D isotopic exchange was shown to strengthen covalent D-O bond within the water molecule^{1,7,8} as well as the non-covalent deuterium bonding^{7,9,10} compared to their respective H-analogs. Stronger intramolecular deuterium bonds strengthen hydrophobic interactions, which in-turn rigidify native structures of proteins and increase their tendency to aggregate in D₂O.¹¹⁻¹⁴

B. Effect of heavy water on phospholipid bilayers: longer lasting hydrogen bonds between the phospholipid headgroups

Studies describing D₂O effect on biological membranes are scarce and mostly focused on the function of membrane proteins, like Na⁺-K⁺ ATPase, Na⁺-H⁺ antiporter, or calcium voltage dependent channels.^{4,15-20} Better understanding of D₂O influence on lipid bilayer is provided by experiments using model membranes and theoretical studies. Under physiological conditions, lipid bilayers are immersed in water media and thus fully hydrated. Water molecules penetrate the headgroup region all the way to phosphate and carbonyl oxygens²¹ and connect the lipid molecules via hydrogen bond network.^{22,23} Replacement of H₂O by D₂O strengthens this network, which results in a number of alterations in properties of the phospholipid bilayers.²⁴⁻²⁹ Differential scanning calorimetry (DSC) data suggests stronger packing of hydrocarbon chains²⁴ and lateral compression accompanied by stabilization of the bilayer at interfacial region²⁷. Combination of DSC and electron spin resonance (ESR) measurements revealed ordering and restricted mobility at the phospholipid headgroups induced by D₂O.²⁶ Recent molecular dynamic (MD) simulations by Róg et al.³⁰ give a comprehensive molecular picture of isotopic effects in zwitterionic phospholipid bilayers. The authors postulated that while time averaged properties, like area per lipid, membrane thickness, headgroup tilt or number of water molecules interacting with the phospholipids were almost unaffected by replacing H₂O by D₂O, the time-dependent properties were altered significantly. Heavier mass and stronger D-bonds compared to H-bonds resulted in a substantially slower mobility of heavy water molecules associated with phospholipid bilayers and more stable (i.e. longer lived) lipid-D₂O and lipid-lipid interactions. Recently, we confirmed these computational predictions by a combination of fluorescence techniques, i.e., fluorescence anisotropy, fluorescence correlation spectroscopy, and TDFS measurements.³¹ The results obtained by the latter technique will be further elaborated on in this contribution.

C. Effect of ions on phospholipid bilayers: do fluoride anions disrupt the hydrogen bond network between the phospholipid headgroups?

When studying structural properties of light or heavy water, effects of ions are hard to overlook, since their presence can either destabilize or stabilize local hydrogen bond networks around them.³² Specific interactions of different salts with biomolecules have been studied since the pioneering works of Franz Hofmeister,^{33, 34} who has ordered the ions according to their ability to precipitate proteins. The specific ionic effects in lipid membranes can be emphasized by tuning the charge of the membrane.³⁵⁻³⁷ E.g. the addition of 20 mol% of negatively charged POPS to POPC bilayer helps to enhance the effects of monovalent cations.³⁸ Similarly, the introduction of the positive charge enhances binding of anions and underlines their specificity.^{35, 37} Our recent study³⁹ applying the TDFS method reported strong adsorption of weakly hydrated ions (Br^- , ClO_4^- and SCN^-) to cationic bilayers accompanied by membrane compression and hindered headgroup mobility. The strongly hydrated fluoride and acetate ions behaved in the opposite way, leading to increased lipid mobility within the headgroup region of the cationic bilayer. We hypothesized that this could have been the effect of disruption of the local hydrogen bond network present at the lipid headgroup region caused by the strongly hydrated anions. This hypothesis is tested in the present work. As explained below, TDFS method is particularly suitable for the study of the presence and duration of the hydrogen bonds within the phospholipid headgroup region.

D. What can we learn on the hydrogen-bonding network between the phospholipid headgroups by probing time-dependent fluorescence shift of Laurdan?

The TDFS technique induces an ultrafast change in the dipole moment of the chromophore via electronic excitation, to which the chromophore's solvation shell is forced to respond. That response can be monitored by a time-dependent shift of the peak maximum of time-resolved emission spectra (TRES), $\nu(t)$. The analysis of $\nu(t)$ reveals independently information on the polarity (total amount of fluorescence shift $\Delta\nu = \nu(0) - \nu(\infty)$ is linearly proportional to a polarity function⁴⁰) and mobility (TDFS kinetics expressed as mean integrated relaxation time, $\tau_r = \int_0^\infty [(\nu(t) - \nu(\infty))/\Delta\nu] dt$ depends on the solvent viscosity of the solvation shell).⁴¹ In phospholipid bilayers, TDFS was determined using a series of amphiphilic compounds, the chromophores of which probe the polarity and mobility at the level of a particular lipid segment along the z-axis of the bilayer. The most common of these dyes and their location in the phospholipid bilayer are depicted in Fig. 2 of Ref. ⁴² and in Fig. 4 of Ref. ⁴³. Here, we will focus on 6-lauroyl-2-dimethylaminonaphthalene (Laurdan). Laurdan is certainly the most widely used of such compound.⁴⁴ Since the steep hydration gradient along the z-axis of the lipid bilayer governs the read-out parameters $\Delta\nu$ and τ_r of an individual membrane probe,⁴⁵ the knowledge of the precise chromophore location is crucial for the interpretation of the TDFS. Regarding Laurdan, all-atom classical MD simulations yielded mean distances of the Laurdan fluorophore from the DOPC bilayer center of $12.3 \pm 2.1 \text{ \AA}$ and $13.5 \pm 2.5 \text{ \AA}$, for ground and excited states, respectively.⁴⁶ The relocation of the chromophore in the excited state occurs on the nanosecond time-scale. Wavelength-dependent quenching experiments with spin-labeled lipids confirm the predictions that Laurdan is located close to the DOPC *sn*-1 carbonyls; the corresponding values of 9.9 \AA and 12.0 \AA were obtained for emission at 420 nm and 530 nm, respectively, resulting in a mean distances from the DOPC bilayer center of $11.4 \pm 2.0 \text{ \AA}$ at 20 °C.

TDFS in the liquid-crystalline phase of lipid bilayers occurs exclusively on the nanosecond time scale.⁴⁵ In bulk water, the process is about 1000 times faster. The residence time of bound water within phospholipid headgroups was shown to be longer than 60 ns.⁴⁷ The TDFS is by theory attributed to the collective relaxation of the dye environment providing no direct information about exchange of single water molecules.⁴⁸ Considering these facts and the location of Laurdan chromophore within bilayers, one can conclude that Laurdan TDFS kinetics reflects predominantly the rearrangement of the hydrated *sn*-1 carbonyl of a DOPC bilayer in the liquid-crystalline phase, while Δv mirrors the polarity at this probed site which is closely related to the level of hydration of the DOPC *sn*-1 carbonyl.⁴² The local dynamics of the lipid carbonyls is largely governed by the local hydrogen bond network created by carbonyls and water molecules.^{30,31} In the present paper we show how this dynamics can be affected by the presence of heavy water and fluoride anions. We also parallel the TDFS results with MD simulations,⁴⁹ which help to understand the experimentally observed interactions between lipids, solvents, and ions.

II. MATERIALS AND METHODS

A. Materials

1,2-dioleoyl-*sn*-glycero-3-phosphocholine (DOPC) and 1,2-dioleoyl-3-trimethylammoniumpropane (DOTAP) were purchased from Avanti Polar Lipids, Inc. (Alabaster, USA). 6-lauroyl-2-dimethylaminonaphthalene (Laurdan) was obtained from Molecular Probes (Eugene, USA). D₂O (99.9% D) and salts, both with purity $\geq 99\%$, were purchased from Sigma Aldrich (St. Louis, USA). Organic solvents of spectroscopic grade were supplied by Merck (Darmstadt, Germany). All chemicals were used without further purification.

B. Sample preparation

Salt solutions were prepared either in Mili Q (Milipore, USA) water or in D₂O. Appropriate volumes of stock solutions of lipids (in CHCl₃) and fluorescent probes (in CH₃OH) were mixed in glass tubes to yield a final concentration in vesicular dispersion of 1.0 mM and 0.01 mM, respectively. Solvents were evaporated under the stream of nitrogen, while heated, and left in the vacuum for at least 2 h in order to remove residual organic solvent. The dry lipid film was suspended in 1.5 ml of a salt solution or water and vortexed for 4 min or until the lipid film was dissolved. Large unilamellar vesicles (LUVs) were formed by extrusion through the 100 nm pore diameter membrane filters (Avestin, Ottawa, Canada).

C. Time-dependent fluorescent shift experiments

A detailed description of the method can be found in ⁴². Theoretical background and the definition of the two parameters determined during the analysis of the results are given in Paragraph I.D.

TDFS experiments were performed at 283 K. Samples were equilibrated at least 15 minutes before the measurement. Steady-state emission spectra were measured using Fluorolog-3 spectrofluorometer (model FL3-11; Jobin Yvon Inc., Edison, NJ, USA) equipped with a xenon-arc lamp. Time-resolved fluorescent decays were recorded using a 5000U Single Photon Counting setup using a cooled Hamamatsu R3809U-50 microchannel plate photomultiplier (IBH, UK).

Laurdan was excited at 373 nm with the IBH NanoLed 11 laser diode. The data were collected for a series of wavelengths ranging from 400 nm to 540 nm with a 10 nm step. Additionally, the emission >399 nm cutoff filter was used to eliminate the scattered light. Each decay was fitted with a multi-exponential function using the iterative reconvolution procedure (IBH DAS6 software).

Time-resolved emission spectra (TRES) were reconstructed from the recorded series of fluorescent decays together with the steady-state emission spectrum⁴⁰ and fitted in order to determine position of their maxima in time after excitation, $\nu(t)$. Analysis of $\nu(t)$ decays plotted in wavenumbers yielded two parameters ($\Delta\nu$ and τ_r) as described in section I.D. Intrinsic uncertainties for the TDFS parameters were 50 cm^{-1} for $\Delta\nu$, and 0.05 ns for τ_r .

D. Molecular dynamics

Atomistic-level classical molecular dynamics simulations were employed to study interactions of ions with DOTAP bilayers. The Berger's united-atom force field was used for description of lipids.⁵⁰ Water was modeled employing the SPC model which is the default water force field for Berger's lipid.⁵¹ For D_2O , the SPC-HW model, which effectively accounts for the quantum mechanical difference between H_2O and D_2O within a classical framework, was used which was previously tested in lipid membrane simulations.^{30,31} Parameters for sodium and chloride ions were taken from the GROMACS force field,⁵² while for fluoride anions the force field introduced by Horinek and co-workers was employed.⁵³ Lipid bilayers containing 128 molecules of DOTAP (64 in each leaflet) were simulated. The membranes were hydrated with approximately 4600 molecules of either H_2O or D_2O . In each system, 128 anions (either Cl^- or F^-) were introduced in the water phase in order to neutralize the positive charge of the membrane, corresponding to 1.5 M concentration of anions. Additional 0.16 M of salt ions, either NaCl or NaF, was added. These amounts of ions resulted in the effective 1.66 M concentration of anions (Cl^- or F^-) and 0.16 M concentration of Na^+ cations. Note that in experiments with cationic membranes there is a surplus of anions present in the water phase in order to neutralize the positive charge of the lipids. However, the experimental concentrations of these neutralizing anions are typically relatively low due to a high dilution of lipid vesicles in water. In practice, due to computational costs, such a dilution cannot be achieved in MD simulations. A typical size of the simulation box was $6.4 \times 6.4 \times 7.3 \text{ nm}^3$ with periodic boundary conditions employed. Both Lennard-Jones and short-range electrostatic interactions were cut off at 1 nm, the long-range electrostatics being accounted for by employing the particle-mesh Ewald method.⁵⁴ The pressure of 1 bar was controlled independently in the directions parallel and perpendicular to the membrane with the Parrinello-Rahman pressure coupling scheme employing the coupling constant of 2 ps.⁵⁵ Simulations were performed at the temperature of 310 K controlled using the Nose-Hoover thermostat algorithm with the 1 ps coupling constant.⁵⁶ The lengths of bonds in lipids were kept constant employing the LINCS algorithm and water molecules were kept rigid via the SETTLE method.^{57,58} Simulations were performed with the GROMACS 4.0.7 software package.⁵² Equations of motion were integrated with the 2 fs time step. Each system was simulated for 100 ns. Equilibration was checked by means of the convergence of area per lipid and density profiles. The trailing 20 ns of each trajectory were used for analysis.

III. RESULTS AND DISCUSSION

Ionic effects along with H₂O/D₂O exchange were investigated using TDFS of Laurdan in neutral 1,2-dioleoyl-*sn*-glycero-3-phosphocholine (DOPC) or positively charged 1,2-dioleoyl-3-trimethylammonium-propane (DOTAP) bilayers. These two lipid systems differ only in their headgroups: zwitterionic PC, and cationic TAP; while their double oleic backbones are identical. The results are presented and discussed together with the results of MD simulations both already published (specific ionic effects in cationic bilayers, effects of heavy water on zwitterionic bilayers) and performed within this study (effect of heavy water on cationic bilayer). The salts we use to introduce fluoride or chloride anions to the lipid bilayer were NaCl/NaF (for MD and preliminary TDFS) and CsCl/CsF for TDFS. The reason for the use of the later was a considerably higher solubility of CsF compared with NaF, which allowed us to amplify the ionic effects by using higher salt concentrations. The below discussed results are in agreement with our preliminary study in which sodium salts were used (data not shown).

A. Zwitterionic bilayers – TDFS experiments

Relaxation of the hydrated carbonyls of DOPC liposomes dispersed in water and salt solutions was monitored using Laurdan TDFS. All the solutions were prepared in either H₂O or D₂O. The obtained results are presented as two parameters $\Delta\nu$ and τ_r separating polarity from the mobility of the polar environment of the probe, respectively. Both parameters for all the measured systems are depicted in Fig. 3. Examples of the original relaxation curves – positions of the time-resolved emission spectra (TRES) are shown in Fig. 2. In all of the studied samples, exchange of water with heavy water resulted in increased values of the integrated relaxation time, τ_r (Fig. 3 A). Relaxation time increased by ~20% in the case of pure water and 1M CsCl and by ~15% for 1M CsF. Similar τ_r increase was observed at lower salt concentration, i.e., ~20% for both 0.15 M NaCl and 0.15 M NaF (data not shown). These results demonstrate the hindrance of the carbonyl mobility of DOPC bilayers. When we take into account the presence of the local hydrogen bonds network created by water and lipid molecules (in this case mainly lipid carbonyls), we can conclude that deuteration of water clearly prolongs the average lifetime of these hydrogen bonds. This effect was already observed in our previous study specifically devoted to the influence of D₂O on the properties of phosphatidylcholine membranes.³¹ Namely, we showed that heavy water increased relaxation time by ~15% in POPC (at 283 K in 10 mM Hepes, pH 7.4, 0.1 mM EDTA) and DMPC (at 310 K in 10 mM Hepes, pH 7.4, 140 mM NaCl, 10 mM KCl, 0.5 mM EDTA). It is worth mentioning that this significant hindrance of local mobility is difficult to probe with other techniques, e.g., the lateral lipid diffusion in both systems was not influenced by water deuteration.³¹

Unlike τ_r , the changes in the total spectral shift ($\Delta\nu$) of Laurdan (Fig. 3 B), reflecting the hydration/polarity of lipid carbonyls, were all within the experimental error of this parameter (~50 cm⁻¹). A visible trend suggesting a slightly decreased polarity upon H₂O/D₂O exchange (~30 cm⁻¹ in average) was nevertheless observed in our previous study performed at the same temperature for a more rigid POPC bilayer, for which a significant $\Delta\nu$ decrease was detected (140 cm⁻¹).³¹ The changes in $\Delta\nu$ probed in lipid bilayers are commonly interpreted in terms of their hydration, since the polarity is there mainly given by the water molecules that hydrate the lipids. Such interpretation is, however, not always valid. Indeed, we have identified number of cases where other polarity affecting factors can be responsible for the changes in the measured $\Delta\nu$.⁵⁹ The dipole moment of D₂O is slightly higher than that of H₂O. Thus, one would not expect any decrease of $\Delta\nu$ solely upon deuteration of water molecules of the hydration shell of a probe. This is a good reason to interpret

the previously observed $\Delta\nu$ decrease as dehydration of lipid carbonyls, especially since it was accompanied by a slight compression of the membrane observed in MD.³¹ Recent TDFS studies of pure isotropic liquids have shown that $\Delta\nu$ measured for N-methyl-6-oxyquinolinium betaine dissolved in pure D₂O was smaller than in H₂O.⁶⁰ We cannot exclude that such specific differences between D₂O and H₂O can also affect the $\Delta\nu$ probed in lipid bilayers.

The above discussed results are in a very good agreement with MD simulations performed by Róg et al., who showed that while heavy water has only a small influence on the structure of DPPC bilayer, it considerably slows down the dynamics of the interactions between the solvent and the lipids.³⁰ It is striking that the persistences of H/D bonds between lipids and water molecules and water bridges between two lipids, as observed in MD, correlate with the measured relaxation time of Laurdan.³¹ More specifically, temperature-dependent D₂O/H₂O experiments together with MD simulations demonstrate that Laurdan τ_r reports on the lifetime of the hydrogen bonds bridging the headgroups of two lipid molecules. At the same time the membrane structure, e.g., order parameter measured by DPH anisotropy, was almost unaffected by D₂O.³¹

To the best of our knowledge, the salt effects in lipid bilayers upon H₂O/D₂O exchange have not been directly addressed so far. In the present study these effects are clearly noticeable (Fig. 3 A). While relaxation times measured for pure water and for 1 M CsCl are very similar to each other, presence of 1 M CsF hinders the mobility probed at lipid carbonyls. This is true for both H₂O and D₂O systems. In our previous studies, adsorption of cations to lipid bilayers was often linked to increase in relaxation time due to formation of ion bridges between lipids.³⁸ However, chloride and fluoride anions are not expected to interact with phosphatidylcholine bilayer.³⁹ Thus, we attribute the presently observed hindrance of the carbonyl mobility to the action of cesium cations. The surprising fact that this effect is only observed for CsF and not for CsCl suggests that the stronger ion pairing between Cs⁺ and Cl⁻, in comparison with that of Cs⁺ and F⁻, prevents penetration of Cs⁺ to lipid carbonyls. Although the presence of CsF influences individual τ_r values, the shift upon H₂O/D₂O exchange is conserved indicating that solvent and ionic effects are independent of each other. Finally, polarity probed by Laurdan is not affected by the salts (Fig. 3 B).

B. Cationic bilayers – TDFS experiments

We have shown that a positively charged lipid bilayer attracts anions revealing their specific interactions with lipids.³⁹ Here, we study TDFS of Laurdan in DOTAP vesicles dispersed in the same solutions as those used for DOPC samples described above. Due to pronounced adsorption of chloride ion, followed by aggregation of DOTAP vesicles, concentration of salts had to be decreased to 0.5 M. It should be mentioned that the positive charge of DOTAP molecules we used is compensated by chloride counterions, thus there is always additional 1 mM chloride in all these samples. The samples were checked for monodispersity using dynamic light scattering (DLS) and no signs of aggregation was detected. Analogous to neutral membranes, cationic bilayers in pure water exhibit restriction of carbonyl group mobility upon H₂O/D₂O exchange. The effect is in this case even more pronounced with a ~30% increase of τ_r (Fig. 3 C).

Ionic effects in DOTAP membranes are clearly much more pronounced than in DOPC. This is likely due to electrostatic attraction between trimethylammonium-propane headgroups (TAP) and anions. Our previous study showed that adsorption of chloride anions slows down the mobility of the carbonyls of DOTAP when dispersed in NaCl or KCl solutions.³⁹ The same is observed here for 0.5 M CsCl both in H₂O and D₂O solutions for which τ_r increases by ~20%. The mobility hindrance upon the H₂O/D₂O exchange persists; τ_r increases by ~25%. The measured polarity was affected

neither by CsCl nor by D₂O (Fig. 3 D). Not even the small decrease of Δv upon water deuteration observed in DOPC was noticed for DOTAP.

The influence of CsF on the relaxation time measured in DOTAP bilayer is the opposite to that of CsCl; ~25% and 40% decrease for H₂O and D₂O, respectively. This is in line with the elevated carbonyl mobility previously detected in DOTAP vesicles dispersed in 0.15 M NaF.³⁹ Interestingly, CsF cancels the τ_r difference between H₂O and D₂O. This observation confirms our hypothesis proposed in the previous study that fluoride anions, when adsorbing to lipid bilayer, can disturb water-lipid interactions by breaking the local hydrogen bond network.³⁹ Once the local H-bond or D-bond network is broken, local mobility at the carbonyl level probed by Laurdan is considerably faster and, consequently, difference between H₂O and D₂O containing systems is no longer observed. Adsorption of fluoride can only be achieved in cationic membranes. This is because adsorption of such a strongly hydrated ion to a hydrophobic interphase involves the loss of some of its hydrating water molecules, which is unfavorable,⁶¹ and has to be counterbalanced by electrostatic attractions with cationic headgroups. This is why the effect of the hydrogen bond breakage by fluoride was not observed in DOPC vesicles. The presence of CsF also decreases polarity at DOTAP carbonyls (Fig. 3 D). This effect, which was already observed for NaF, was attributed to water “stealing” by F⁻, i.e., the tight binding of water molecules to F⁻ changes their rotational mobility and makes them less active in the probed relaxation process.³⁹

C. Cationic bilayers – MD simulations

To further characterize the above-described effects of heavy water and salt ions on the properties of cationic lipid bilayer, we performed MD simulations mimicking the experimental systems. In MD simulations, we observe that overall structural properties of the investigated DOTAP bilayers are not very sensitive to the type of investigated anion (Cl⁻ vs F⁻) or water (H₂O vs D₂O). Namely, the area per lipid (APL) for the studied membrane is the same within the error bars for all systems, ranging from 0.62 to 0.64 (± 0.01) nm². APL which reflects lateral compactness of lipid membranes is typically altered by the change of the membrane environment (e.g., by the type of salt)³⁸. We have shown previously that APL is often inversely proportional to the TDFS relaxation time.^{38, 49} In the present case, however, the changes in τ_r are not reflected in APL. As we show further, the reason for the longer relaxation times in D₂O observed here are not connected with structural alterations, but rather with the dynamics of the hydrogen bonds between the lipids and D₂O. Fig. 4 depicts density profiles of selected membrane components along the bilayer normal. In all cases, the structure of the bilayer, in particular, location of both DOTAP carbonyl groups and headgroups is virtually the same. Similarly, the penetration depth of the investigated anions (Cl⁻ and F⁻) is the same in all systems. The anions are adsorbed at the outer region of the water-membrane interface and preferentially localized in the vicinity of the cationic DOTAP headgroups. There is also certain overlap between the density profiles of ions and the carbonyl groups of DOTAP acyl chains. Na⁺ cations preferentially reside in the water phase with a minor penetration into the bilayer. A somewhat different behavior can be observed in the system with H₂O and NaF where Na⁺ ions accumulate at the very outer parts of the water membrane interface because of the tendency of Na⁺ to form relatively strong ion pairs with F⁻. Nevertheless, it is reasonable to assume that due to low concentration of cations the influence of Na⁺ on the bilayer can be neglected. Penetration of water (both H₂O and D₂O) into the membrane is similar in all cases. Water penetrates relatively deep into the membrane, interacting with both TAP⁺ and carbonyl groups of DOTAP. We monitored interactions of water with lipids by means of radial distribution

functions (RDF). In Fig. 5 A, RDFs calculated between carbonyl groups of the *sn*-2 acyl chains of DOTAP and oxygen atoms of water are shown. The peaks located at approximately 0.27 nm correspond to preferential water-carbonyl contacts occurring due to hydrogen bonds formation between either H or D atoms of water and carbonyl groups of lipids. There is virtually no difference between the systems studied. Small differences between the RDF curves at longer distances are addressed further in the text. Fig. 5 B depicts RDFs between *sn*-2 carbonyl groups of different lipid molecules and represents inter-lipid binding. The curves are similar for all systems confirming thus that the structure of the DOTAP membrane in the region occupied by carbonyl groups is not sensitive to the ion and water type.

The lack of significant structural differences between cationic bilayers hydrated with H₂O or D₂O observed here is in agreement with previous experimental and simulation studies of neutral membranes.^{30,31} At the same time, those studies demonstrated that the bilayer dynamics is significantly altered by D₂O. To address time-dependent properties of the bilayers, we analyzed autocorrelation functions of contacts between water and lipid atoms. In Fig. 6 A, B autocorrelation curves for carbonyl–hydrogen (or carbonyl–deuterium) and carbonyl–carbonyl contacts are shown. The time scale of the carbonyl–water binding is in the range of one nanosecond whereas the timescale of carbonyl–carbonyl interactions is in the ten-nanosecond range at least. In both carbonyl–water and carbonyl–carbonyl cases, the dynamics is slower in D₂O with compared to H₂O. This finding is in agreement with the mobility of the carbonyls probed by Laurdan TDFS. Satisfactorily, also the timescale of the carbonyl-carbonyl and carbonyl-water interactions agrees very well with the TDFS kinetics (please compare Fig. 2 and Fig. 6). The obtained TDFS relaxation times (0.5-1.1 ns) are in the range of the correlation times obtained in MD for carbonyl-carbonyl (3-4 ns) and carbonyl-water (0.03-0.11 ns) interactions. The observed retardation of bond breaking in D₂O is in agreement with previous studies of zwitterionic membranes in H₂O and D₂O where hindering of membrane kinetics was observed in heavy water.^{30,31} MD correlation curves show no significant differences between F⁻ and Cl⁻; only in the case of carbonyl–carbonyl contacts the presence of F⁻ hinders the binding kinetics slightly more than Cl⁻. This small difference is, however, inconsistent with the TDFS results showing increased carbonyl mobility in the presence of fluoride, possibly pointing to certain force field inaccuracies, particularly for F⁻.

As demonstrated in Fig. 4, anions preferentially occupy the region of the TMA⁺ moiety of DOTAP. The contacts between TMA⁺ and anions are quantified by RDFs presented in Fig. 7 A. There is a significant difference between interactions of TMA⁺ with either of the two ions. Namely, the RDF peak calculated for TMA⁺-Cl⁻ pairs is narrower and higher than that for TMA⁺-F⁻. These results demonstrate that F⁻ is able to interact with TMA⁺ groups at shorter distances than Cl⁻ (due to relatively small ionic radius of F⁻). However, in the interionic distance terms, the TMA⁺-F⁻ interactions are more flexible than that of TMA⁺-Cl⁻. A visual inspection of the trajectories reveals that anions are relatively well hydrated while interacting with the bilayers. Cl⁻ interacts mainly by direct contacts with TMA⁺. In the case of F⁻, the hydration shell is relatively tight and, consequently F⁻ frequently forms water separated ion pairs with TMA⁺. These two modes of TAP⁺ binding by F⁻ are reflected by the structured character of the TMA⁺-F⁻ RDF function (Fig. 7 A) with the peak at ~0.4 nm corresponding to direct TAP⁺-F⁻ contacts and the maximum at ~0.6 nm present due to water-separated configurations. In the case of Cl⁻, which has a more flexible hydration shell, such an effect is not present and the direct TMA⁺-Cl⁻ configurations prevail. Notably, the ionic effect regarding the TMA⁺ binding is stronger than the influence of the water type as the RDFs do not differ appreciably between H₂O and D₂O. Note that in the case of halide anions, the use of polarizable force fields can lead to somewhat stronger anion-membrane binding

than that observed in non-polarizable ones [<http://pubs.acs.org/doi/abs/10.1021/jp102389k>]. This effect, however, is the most significant for the large and polarizable Γ^- anions and we do not expect it to play a key role in the case of Cl^- and, in particular, relatively small F^- . Regarding the dynamics, as evident from the autocorrelation curves in Fig. 6 C, in D_2O the breaking of TMA^+ -anion contacts is slower than in H_2O . In addition, the kinetics is slower in the presence of F^- compared to that observed for Cl^- . This could be rationalized by a less flexible environment of the more tightly hydrated F^- .

Hydration of the DOTAP bilayer in the region of TMA^+ groups is somewhat elevated in the NaF solution compared to NaCl (see Fig. 7B). This effect is caused by the tendency of F^- to bring its tightly bound hydration shell close to the bilayer. Note, that such an elevated hydration was not detected in TDFS experiment. In fact $\Delta\nu$ is even decreased in CsF solution. This is likely because the tightly bound water molecules that hydrate fluoride ion do not contribute to the relaxation probed by Laurdan. The kinetics of TMA^+ -water contacts is slowed down in D_2O (see Fig. 6 D). It is also slightly slower in the presence of F^- . The latter result stems again from the tight hydration shell of fluoride anions.

SUMMARY AND CONCLUSIONS

Our combined TDFS and MD study demonstrates a number of effects of heavy water and halide anions on the properties of cationic and zwitterionic lipid bilayers. Most importantly:

- 1) Heavy water significantly slows down lipid mobility in the zwitterionic (DOPC) as well as in the cationic (DOTAP) model lipid membranes. This is observed experimentally at the level of lipid carbonyls probed by TDFS of Laurdan in DOPC and DOTAP in pure water, NaCl, CsCl, NaF, and CsF solutions. TDFS results obtained for DOPC confirm the existence of prolonged lifetime of PC-water and PC-PC water bridges, which was previously predicted by simulations for DPPC bilayer in D_2O .³⁰ The TDFS results obtained for DOTAP are in full agreement with the results of the present MD simulations. Namely, DOTAP membranes in NaCl, and NaF solutions show longer lived D-bonding at both the carbonyls and the TAP^+ headgroups of DOTAP.
- 2) As opposed to the dynamical properties mentioned in point 1, the structure of DOTAP membrane assessed with MD, is not significantly affected by water deuteration. The herein simulated cationic DOTAP bilayer also behaves in this respect similarly to the previously investigated zwitterionic DPPC.³⁰
- 3) The presence of chloride and fluoride salts does not alter deuteration effects measured by Laurdan TDFS in DOPC bilayer. A somewhat hindered mobility that we associate with Cs^+ bridges between lipid carbonyls is observed for CsF both in H_2O and D_2O .
- 4) In cationic membrane, experiments indicate that F^- is able to disrupt local hydrogen bonding to the point where the DOTAP carbonyl mobilities in D_2O and H_2O are no longer distinguishable by Laurdan TDFS. While MD results do not confirm this finding, they clearly show differences in the binding of F^- and Cl^- to the cationic headgroup of DOTAP, i.e., direct binding of Cl^- vs. a mixture of direct and solvent-separated ion pairing of F^- .
- 5) MD simulations of both F^- (due to its high charge density) and D_2O (due to only phenomenological inclusion of isotope effects) suffer from imperfections of the force-field used. The fluoride ions in D_2O , are problematic to describe in the framework of classical force fields due to two reasons. First, it was demonstrated recently by *ab initio* path integral simulations that even in H_2O , the nuclear quantum effects play an important role and, for

instance, lead to non-monotonous change of the length of fluoride-H₂O hydrogen bonds when going from one- to three-water clusters [<http://pubs.acs.org/doi/pdf/10.1021/jp403295h>]. This phenomenon is particularly important in the case of fluoride-membrane interactions where F⁻ forms hydrogen bonds with one to few waters in the relatively dehydrated region of carbonyl groups of lipids. Second, nuclear quantum effects cause structural differences between fluoride-H₂O and fluoride-D₂O as recently shown by employing path integral hybrid Monte Carlo simulations [<http://scitation.aip.org/content/aip/journal/jcp/132/14/10.1063/1.3367724>]. These two examples demonstrate that classical force fields, which include nuclear effect only implicitly, have intrinsic difficulties with full description of D₂O-F⁻ systems. In the present work, this problem emerged in the case of the DOTAP-F⁻ system.

The above presented results demonstrate the importance of hydrogen bonding between the solvent and carbonyls or headgroups of lipid bilayers. Use of model membranes composed of a synthetic cationic lipid enabled adsorption of the highly hydrated fluoride anion that replaced the water bridges between the lipids. This, in turn, resulted in the observed increase of the mobility of DOTAP carbonyls. Experimental studies on the local hydrogen bonding network in liquid crystalline membranes like lipid bilayers are very demanding. Here we show that TDFS method can be successfully applied to characterize the dynamics of those bonds. Moreover, not only H₂O/D₂O exchange, but also introduction of strongly hydrated ions can be valuable experimental tool, in studying and controlling hydration of biological macromolecular assemblies.

ACKNOWLEDGEMENTS

Financial support was provided by the Czech Science Foundation (grant P208/12/G016). The Academy of Sciences of the Czech Republic is acknowledged for Praemium Academie awards (MH and PJ). PJ acknowledges the Academy of Finland for the FiDiPro award.

REFERENCES

- 1 G. Nemethy and H. A. Scheraga, *J Chem Phys* **41**, 680 (1964).
- 2 C. S. Pittendrigh, P. C. Caldarola, and E. S. Cosbey, *Proc Natl Acad Sci U S A* **70**, 2037 (1973).
- 3 V. G. Bruce and C. S. Pittendrigh, *J Cell Comp Physiol* **56**, 25 (1960).
- 4 D. J. Kushner, A. Baker, and T. G. Dunstall, *Can J Physiol Pharmacol* **77**, 79 (1999).
- 5 W. H. Adams and D. G. Adams, *Journal of Pharmacology and Experimental Therapeutics* **244**, 633 (1988).
- 6 J. Lamprecht, D. Schroeter, and N. Paweletz, *J Cell Sci* **98**, 463 (1991).
- 7 D. Wade, *Chem Biol Interact* **117**, 191 (1999).
- 8 K. B. Wiberg, *Chem Rev* **55**, 713 (1955).
- 9 L. Benjamin and G. C. Benson, *J Phys Chem* **67**, 858 (1963).
- 10 S. Scheiner and M. Cuma, *J Am Chem Soc* **118**, 1511 (1996).
- 11 P. Cioni and G. B. Strambini, *Biophys J* **82**, 3246 (2002).
- 12 G. C. Kresheck, H. Schneider, and H. A. Scheraga, *J Phys Chem* **69**, 3132 (1965).
- 13 M. J. Parker and A. R. Clarke, *Biochemistry* **36**, 5786 (1997).
- 14 P. Sasisanker, A. Oleinikova, H. Weingartner, R. Ravindra, and R. Winter, *Phys Chem Chem Phys* **6**, 1899 (2004).
- 15 P. R. Andjus, A. A. Kataev, A. A. Alexandrov, D. Vucelić, and G. N. Berestovsky, *J Membr Biol* **142**, 43 (1994).
- 16 P. R. Andjus and D. Vucelic, *J Membr Biol* **115**, 123 (1990).

17 C. Elsing, A. Hirlinger, E. L. Renner, B. H. Lauterburg, P. J. Meier, and J. Reichen, *Biochem J* **307** (Pt 1), 175 (1995).

18 B. Prod'hom, D. Pietrobon, and P. Hess, *Nature* **329**, 243 (1987).

19 S. Vasdev, I. P. Gupta, C. A. Sampson, L. Longerich, and S. Parai, *Can J Cardiol* **9**, 802 (1993).

20 S. Vasdev, V. M. Prabhakaran, M. Whelan, C. A. Ford, L. Longerich, and S. Parai, *Artery* **21**, 124 (1994).

21 J. Grdadolnik, J. Kidrič, and D. Hadži, *Chem Phys Lipids* **59**, 57 (1991).

22 M. Pasenkiewicz-Gierula, Y. Takaoka, H. Miyagawa, K. Kitamura, and A. Kusumi, *J. Phys. Chem. A* **101**, 3677 (1997).

23 V. V. Volkov, Y. Takaoka, and R. Righini, *J Phys Chem B* **113**, 4119 (2009).

24 C. H. Chen, *J Phys Chem-U*s **86**, 3559 (1982).

25 G. Lipka, B. Z. Chowdhry, and J. M. Sturtevant, *J. Phys. Chem* **88**, 5401 (1984).

26 L. D. Ma, R. L. Magin, G. Bacic, and F. Dunn, *Biochim Biophys Acta* **978**, 283 (1989).

27 H. Matsuki, H. Okuno, F. Sakano, M. Kusube, and S. Kaneshina, *Biochim Biophys Acta* **1712**, 92 (2005).

28 J. Milhaud, E. Hantz, and J. Liquier, *Langmuir* **22**, 6068 (2006).

29 K. Ohki, *Biochem Biophys Res Commun* **174**, 102 (1991).

30 T. Róg, K. Murzyn, J. Milhaud, M. Karttunen, and M. Pasenkiewicz-Gierula, *J Phys Chem B* **113**, 2378 (2009).

31 L. Beranová, J. Humpolíčková, J. Sýkora, A. Benda, L. Cwiklik, P. Jurkiewicz, G. Gröbner, and M. Hof, *Phys Chem Chem Phys* **14**, 14516 (2012).

32 H. J. Bakker, *Chem Rev* **108**, 1456 (2008).

33 F. Hofmeister, *Archiv Experimentelle Pathologie und Pharmakologie* **25**, 1 (1888).

34 W. Kunz, J. Henle, and B. W. Ninham, *CURRENT OPINION IN COLLOID & INTERFACE SCIENCE* **9**, 19 (2004).

35 J. J. Garcia-Celma, L. Hatahet, W. Kunz, and K. Fendler, *Langmuir* **23**, 10074 (2007).

36 A. A. Gurtovenko, M. Miettinen, M. Karttunen, and I. Vattulainen, *The Journal of Physical Chemistry B* **109**, 21126 (2005).

37 P. M. Macdonald and J. Seelig, *Biochemistry* **27**, 6769 (1988).

38 P. Jurkiewicz, L. Cwiklik, A. Vojtíšková, P. Jungwirth, and M. Hof, *Biochim Biophys Acta* **1818**, 609 (2012).

39 S. Pokorna, P. Jurkiewicz, L. Cwiklik, M. Vazdar, and M. Hof, *Faraday Discuss* **160**, 341 (2013).

40 M. L. Horng, J. A. Gardecki, A. Papazyan, and M. Maroncelli, *JOURNAL OF PHYSICAL CHEMISTRY* **99**, 17311 (1995).

41 R. Richert, F. Stickel, R. S. Fee, and M. Maroncelli, *Chemical Physics Letters* **229**, 302 (1994).

42 P. Jurkiewicz, J. Sýkora, A. Olzyńska, J. Humpolíčková, and M. Hof, *J Fluoresc* **15**, 883 (2005).

43 A. P. Demchenko, Y. Mely, G. Duportail, and A. S. Klymchenko, *Biophys J* **96**, 3461 (2009).

44 L. A. Bagatolli, (Springer Berlin Heidelberg, 2013), Vol. 13, p. 3.

45 J. Sykora, P. Kapusta, V. Fidler, and M. Hof, *Langmuir* **18**, 571 (2002).

46 J. Barucha-Kraszewska, S. Kraszewski, P. Jurkiewicz, C. Ramseyer, and M. Hof, *Biochim Biophys Acta* **1798**, 1724 (2010).

47 P. O. Westlund, *Journal of Physical Chemistry B* **104**, 6059 (2000).

48 B. Halle and L. Nilsson, *Journal of Physical Chemistry B* **113**, 8210 (2009).

49 P. Jurkiewicz, L. Cwiklik, P. Jungwirth, and M. Hof, *Biochimie* **94**, 26 (2012).

50 O. Berger, O. Edholm, and F. Jahnig, *Biophysical Journal* **72**, 2002 (1997).

51 H. J. C. Berendsen, J. P. M. Postma, W. F. Van Gunsteren, and J. Hermans, in *Intermolecular Forces* (D. Reidel Publishing Company, Dordrecht, 1981), p. 331.

52 B. Hess, C. Kutzner, D. van der Spoel, and E. Lindahl, *Journal of Chemical Theory and Computation* **4**, 435 (2008).

53 D. Horinek, S. I. Mamatkulov, and R. R. Netz, *The Journal of Chemical Physics* **130**, 124507 (2009).

54 U. Essmann, L. Perera, M. L. Berkowitz, T. Darden, H. Lee, and L. G. Pedersen, The Journal of
Chemical Physics **103**, 8577 (1995).
55 M. Parrinello and A. Rahman, Journal of Applied Physics **52**, 7182 (1981).
56 S. Nose, Molecular Physics **52**, 255 (1984).
57 B. Hess, H. Bekker, H. J. C. Berendsen, and J. G. E. M. Fraaije, Journal of Computational Chemistry
18, 1463 (1997).
58 R. W. Hockney, S. P. Goel, and J. W. Eastwood, J Comput Phys **14**, 148 (1974).
59 M. Hof, Biophys J?, ? (2014).
60 M. Sajadi, M. Weinberger, H. A. Wagenknecht, and N. P. Ernsting, Physical Chemistry Chemical
Physics **13**, 17768 (2011).
61 E. Leontidis and A. Aroti, J Phys Chem B **113**, 1460 (2009).
62 P. Jurkiewicz, A. Olzynska, M. Langner, and M. Hof, Langmuir **22**, 8741 (2006).

FIG. 1

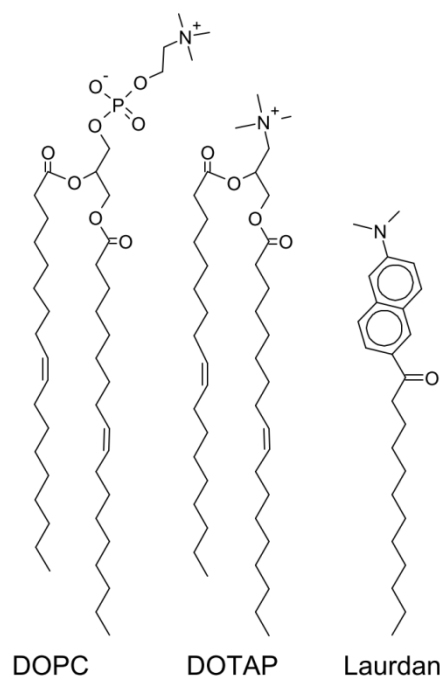


FIG. 1. Position of Laurdan probe within the lipid bilayer.^{46, 62}

FIG. 2

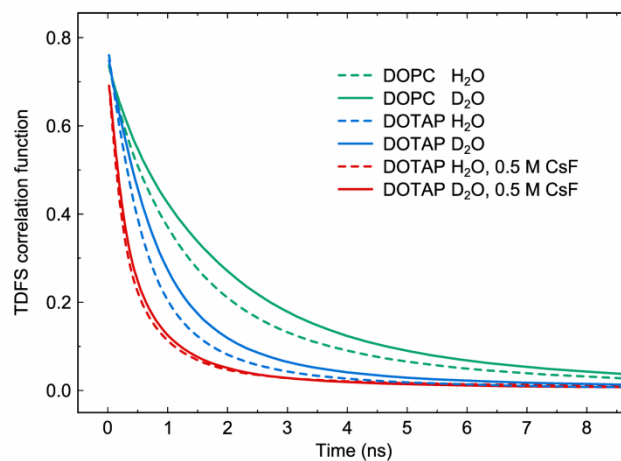


FIG. 2. TDFS correlation functions for Laurdan probing carbonyl region of DOPC and DOTAP vesicles dispersed in H₂O, D₂O, and 0.5 M CsF (both in H₂O and D₂O). Excitation wavelength – 373 nm, temperature – 10 °C.

FIG. 3

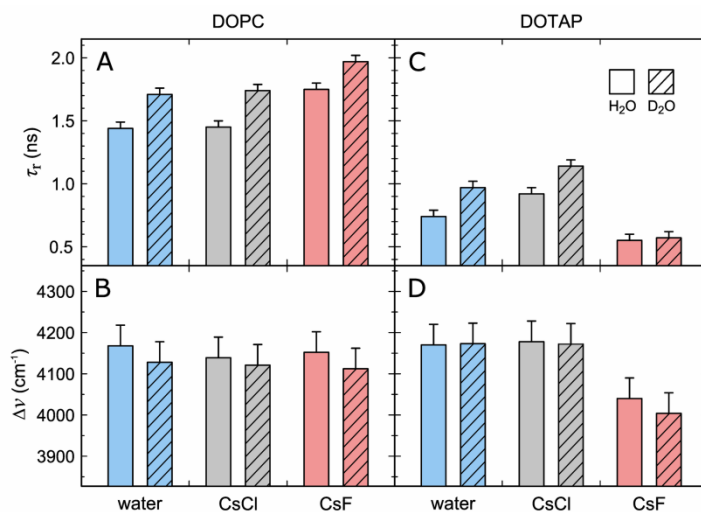


FIG. 3. TDFS parameters: integrated solvent relaxation time (A, C) and total spectral shift (B, D) measured for Laurdan embedded in either zwitterionic DOPC (A, B) and cationic DOTAP (C, D) lipid vesicles. The vesicles were dispersed either in pure water or in CsCl or CsF salt solution (1 M for DOPC, 0.5 M for DOTAP). The solutions were prepared in light or in heavy water. Excitation wavelength – 373 nm, temperature – 10 °C.

FIG. 4

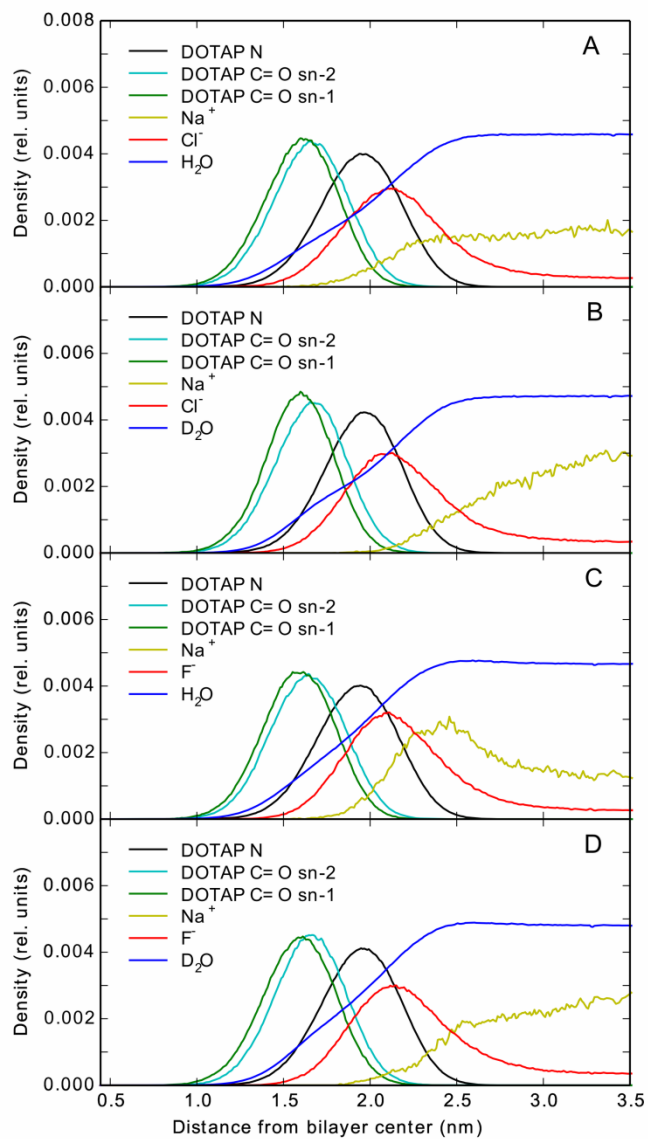


FIG. 4. Density profiles of selected system components along the bilayer normal.

FIG. 5

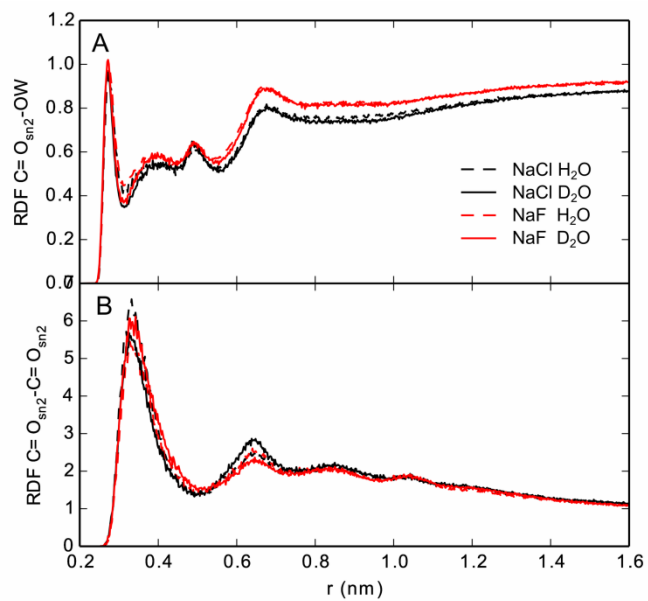


FIG. 5. Radial distribution functions between oxygen atoms of the sn-2 carbonyl groups of DOTAP and water oxygen atoms (A), and between the oxygen of the carbonyl groups (B).

FIG. 6

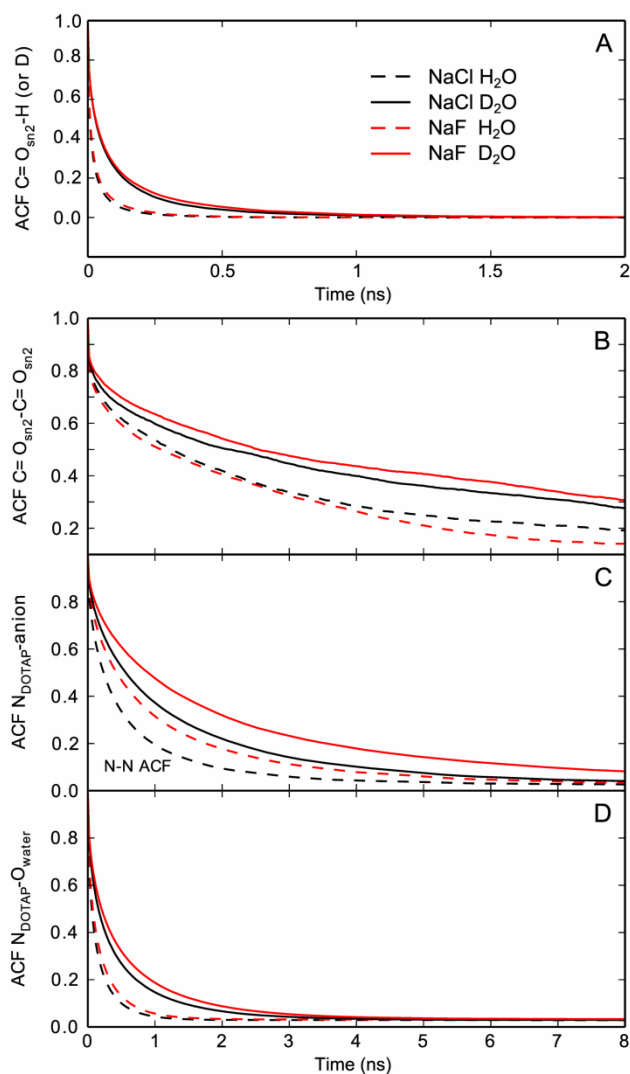


FIG. 6. Time correlation of contacts between: oxygen atoms of the sn-2 carbonyl groups of DOTAP and water oxygen atoms (A), the oxygen atoms of the carbonyl groups (B), nitrogen atoms of the cationic TMA⁺ moiety of DOTAP headgroups and anions (C), nitrogen atoms of the TMA⁺ and water oxygen atoms (D)

FIG. 7

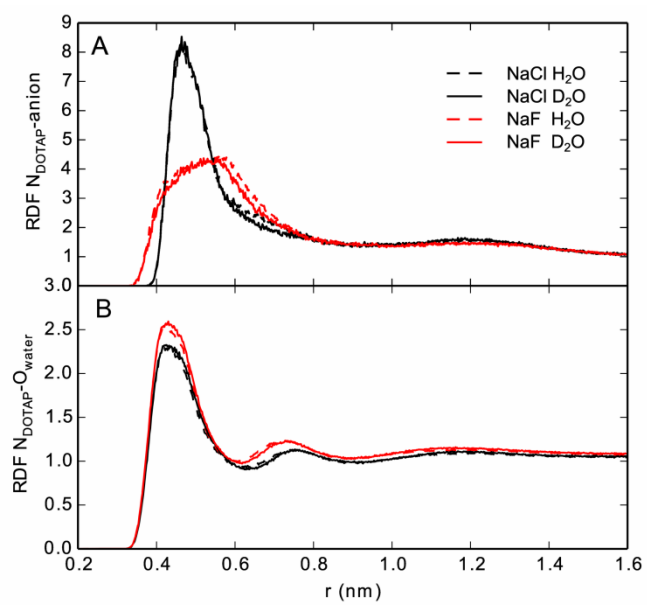


FIG. 7. Radial distribution functions between nitrogen atoms of the cationic TMA⁺ moiety of DOTAP headgroups and anions (A), and water oxygen atoms (B).